

Testing the existence of regions of stable orbits at small radii around black hole candidates

Cosimo Bambi^{1,*} and Georgios Lukes-Gerakopoulos^{2,†}

¹*Center for Field Theory and Particle Physics & Department of Physics, Fudan University, 200433 Shanghai, China*

²*Theoretical Physics Institute, Friedrich-Schiller-Universität Jena, D-07743 Jena, Germany*

(Dated: October 31, 2018)

Black hole candidates in X-ray binary systems and at the centers of galaxies are expected to be the Kerr black holes of General Relativity, but the actual nature of these objects has yet to be verified. In this paper, we consider the possibility that they are exotic compact objects and we describe their exterior gravitational field with a subclass of the Manko-Novikov metrics, which are exact solutions of the vacuum Einstein's equations and can describe the spacetime geometry around bodies with arbitrary mass-multipole moments. We point out that around a Manko-Novikov object there may exist many disconnected non-plunging regions at small radii, with no counterpart in the Kerr background, and that their existence may be tested. For instance, in the presence of an accretion disk, they may be filled by the accreting gas, forming a ring structure that might remind the rings of Saturn. We suggest that the existence of these regions may have a clear observational signature in the waveform of the gravitational radiation emitted by an EMRI: in the last stage of the inspiral, the waveform would be the combination of “regular chirps”, produced when the small object orbits in one of the non-plunging regions, and “bursts”, released when the small object jumps from a non-plunging region to another one at smaller radii. Our conclusions are supported by some numerical calculations of trajectories in the geodesic approximation, in which a particle plunges from the ISCO and then seems to get trapped in the potential well at smaller radii.

PACS numbers: 97.60.Lf, 04.50.Kd, 97.10.Gz

I. INTRODUCTION

In 4-dimensional General Relativity, uncharged black holes (BHs) are described by the Kerr solution and are characterized by only two parameters: the mass, M , and the spin angular momentum, J [1]. Astrophysical BH candidates are stellar-mass compact objects in X-ray binary systems [2] and super-massive bodies at the centers of galaxies [3]¹. The former have a mass exceeding $3 M_{\odot}$ and are therefore too heavy to be neutron or quark stars for any plausible matter equation of state [5]. At least some of the super-massive BH candidates in galactic nuclei turn out to be too heavy, compact, and old to be clusters of non-luminous bodies [6]. These two classes of objects are thought to be the Kerr BH predicted by General Relativity because there is no alternative explanation in the framework of conventional physics. However, their actual nature has yet to be proven [7].

In this work, we consider the possibility that astrophysical BH candidates are exotic compact objects and we describe their *exterior* gravitational field with a subclass of the Manko-Novikov (MN) metrics [8]. The MN spacetimes are exact solutions of the vacuum Einstein's equations and they are characterized by the mass of the compact object, its spin angular momentum, and an infinite

number of deformation parameters, setting all the mass-multipole moments. Previous work on these metrics considered only the simplest case with one deformation parameter, the anomalous mass-quadrupole moment q , assuming zero all the higher anomalous mass moments [9–12]. The existence of some disconnected non-plunging regions at small radii in the MN spacetimes, which have no counterpart in the Kerr BH background (but see [13]), is already known. So far they have been quite ignored and were considered to be of no astrophysical interest. The reason is that it was thought that their orbital energy is always higher than the one at larger radii and therefore that they would be difficult to populate by the gas of the accretion disk or by small bodies inspiralling into the BH candidate. Here we point out that this is not always true and that the existence of such non-plunging regions may have astrophysical implications. Moreover, in addition to a non-vanishing q , we consider the possibility of a non-vanishing anomalous mass-hexadecapole moment h , and we argue that the maximum number of non-plunging regions increases as the number of non-zero deformation parameters increases.

In the Kerr metric, equatorial circular orbits are always vertically stable, while they are radially stable for radii $r > r_{\text{ISCO}}$, where r_{ISCO} is the radius of the innermost stable circular orbit (ISCO). Equatorial circular orbits with radii $r_{\text{PO}} < r < r_{\text{ISCO}}$, where r_{PO} is the radius of the photon orbit, are unstable for small perturbations along the radial direction, while there are no equatorial circular orbits for $r < r_{\text{PO}}$. In non-Kerr spacetimes, equatorial circular orbits may also be vertically unstable, which leads to a number of completely

* bambi@fudan.edu.cn

† ggglukes@gmail.com

¹ The existence of a third class of objects, intermediate-mass BH candidates with $M \sim 10^2 - 10^4 M_{\odot}$, is still controversial, because their detections are indirect, and definitive dynamical measurements of their masses are lacking [4].

new phenomena [12, 14]. In the MN metric with a non-vanishing anomalous quadrupole moment, there may be an island of stable equatorial circular orbits in the region $r < r_{\text{ISCO}}$; that is, there may exist two radii r_1 and r_2 such that equatorial circular orbits with $r_1 < r < r_2$ are stable. If we consider the MN metric with non-vanishing anomalous mass-quadrupole and mass-hexadecapole moment, there may exist two disconnected non-plunging regions for $r < r_{\text{ISCO}}$, say $r_1 < r < r_2$ and $r_4 < r < r_5$. In the presence of an accretion disk, these regions may be filled by the accreting gas, because their energy and angular momentum can be lower than the ones at larger

radii.

Throughout the paper, we use units in which $G_{\text{N}} = c = 1$.

II. MANKO-NOVIKOV SPACETIMES

The MN metrics [8] are stationary, axisymmetric, and asymptotically flat exact solutions of the vacuum Einstein's equations with arbitrary mass-multipole moments. In quasi-cylindrical coordinates (ρ, z) and in prolate spheroidal coordinates (x, y) , the line element is, respectively,

$$\begin{aligned} ds^2 &= -f(dt - \omega d\phi)^2 + \frac{e^{2\gamma}}{f}(d\rho^2 + dz^2) + \frac{\rho^2}{f}d\phi^2 = \\ &= -f(dt - \omega d\phi)^2 + \frac{k^2 e^{2\gamma}}{f}(x^2 - y^2) \left(\frac{dx^2}{x^2 - 1} + \frac{dy^2}{1 - y^2} \right) + \frac{k^2}{f}(x^2 - 1)(1 - y^2)d\phi^2, \end{aligned} \quad (1)$$

where

$$f = e^{2\psi} A/B, \quad \omega = 2ke^{-2\psi} CA^{-1} - 4k\alpha(1 - \alpha^2)^{-1}, \quad e^{2\gamma} = e^{2\gamma'} A(x^2 - 1)^{-1}(1 - \alpha^2)^{-2}, \quad (2)$$

and

$$\psi = \sum_{n=1}^{+\infty} \frac{\alpha_n P_n}{R^{n+1}}, \quad (3)$$

$$\begin{aligned} \gamma' &= \frac{1}{2} \ln \frac{x^2 - 1}{x^2 - y^2} + \sum_{m,n=1}^{+\infty} \frac{(m+1)(n+1)\alpha_m \alpha_n}{(m+n+2)R^{m+n+2}} (P_{m+1}P_{n+1} - P_m P_n) + \\ &+ \left[\sum_{n=1}^{+\infty} \alpha_n \left((-1)^{n+1} - 1 + \sum_{k=0}^n \frac{x-y + (-1)^{n-k}(x+y)}{R^{k+1}} P_k \right) \right], \end{aligned} \quad (4)$$

$$A = (x^2 - 1)(1 + \tilde{a}\tilde{b})^2 - (1 - y^2)(\tilde{b} - \tilde{a})^2, \quad (5)$$

$$B = [x + 1 + (x-1)\tilde{a}\tilde{b}]^2 + [(1+y)\tilde{a} + (1-y)\tilde{b}]^2, \quad (6)$$

$$C = (x^2 - 1)(1 + \tilde{a}\tilde{b})[\tilde{b} - \tilde{a} - y(\tilde{a} + \tilde{b})] + (1 - y^2)(\tilde{b} - \tilde{a})[1 + \tilde{a}\tilde{b} + x(1 - \tilde{a}\tilde{b})], \quad (7)$$

$$\tilde{a} = -\alpha \exp \left[\sum_{n=1}^{+\infty} 2\alpha_n \left(1 - \sum_{k=0}^n \frac{(x-y)}{R^{k+1}} P_k \right) \right], \quad (8)$$

$$\tilde{b} = \alpha \exp \left[\sum_{n=1}^{+\infty} 2\alpha_n \left((-1)^n + \sum_{k=0}^n \frac{(-1)^{n-k+1}(x+y)}{R^{k+1}} P_k \right) \right]. \quad (9)$$

Here $R = \sqrt{x^2 + y^2 - 1}$ and P_n are the Legendre polynomials with argument xy/R ,

$$\begin{aligned} P_n &= P_n \left(\frac{xy}{R} \right), \\ P_n(\chi) &= \frac{1}{2^n n!} \frac{d^n}{d\chi^n} (\chi^2 - 1)^n. \end{aligned} \quad (10)$$

The MN solutions have an infinite number of free parameters: α , which regulates the spin J of the central compact object; k , which regulates the mass M of the central compact object; and α_n ($n = 1, \dots, +\infty$) which

regulate the mass-multipole moments, starting from the dipole α_1 , to the quadrupole α_2 , etc. For $\alpha \neq 0$ and $\alpha_n = 0$, the metric reduces to the Kerr solution. For $\alpha = \alpha_n = 0$, it reduces to the Schwarzschild one. For $\alpha = 0$ and $\alpha_n \neq 0$, we obtain the static Weyl metric.

Without loss of generality, we can put $\alpha_1 = 0$ to bring the massive object to the origin of the coordinate system. In what follows, we restrict our attention to the subclass of MN spacetimes with $\alpha_n = 0$ for $n \neq 2$ and

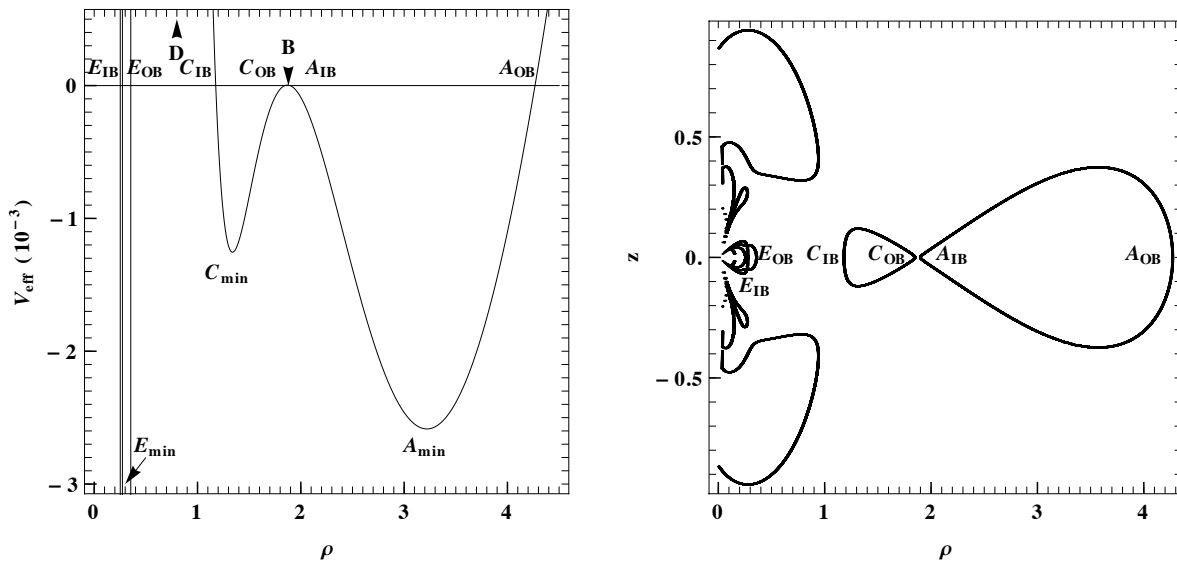


FIG. 1. The left panel shows the profile of the effective potential on the equatorial plane, $V_{\text{eff}}(\rho, z=0)$, for $M = 1$, $a_* = 0.5$, $q = -0.18$, $h = -0.024$, $E = 0.9143$, and $L_z = 2.83$. $V_{\text{eff}} = 0$ (black horizontal line) is the limit of the allowed region. The roots of the effective potential, i.e., A_{OB} , A_{IB} , C_{OB} , C_{IB} , E_{OB} , and E_{IB} , determine the limits of three disconnected regions of bounded non-plunging orbits. The index OB stands for outer border, while IB for inner border. The minima A_{min} , C_{min} , and E_{min} of V_{eff} indicate the existence of stable circular orbits, while the maxima B and D indicate the existence of unstable circular orbits. The right panel shows the limits of the allowed region $V_{\text{eff}} = 0$ on the $\rho - z$ plane, known as CZVs.

⁴². We then have four free parameters (k , α , α_2 , α_4) related to the mass M , the dimensionless spin parameter $a_* = J/M^2$, the anomalous mass-quadrupole moment $q = -(Q - Q_{\text{Kerr}})/M^3$, and the anomalous mass-hexadecapole moment $h = -(H - H_q)/M^5$, where H_q is the mass-hexadecapole moment of the object with $h = 0$ and for $q = 0$ it reduces to $H_{\text{Kerr}} = J^4/M^3$, by the relations

$$\alpha = \frac{\sqrt{1 - a_*^2} - 1}{a_*}, \quad (11)$$

$$k = M \frac{1 - \alpha^2}{1 + \alpha^2}, \quad (12)$$

$$\alpha_2 = q \frac{M^3}{k^3}, \quad (13)$$

$$\alpha_4 = h \frac{M^5}{k^5}. \quad (14)$$

Note that q measures the deviation from the quadrupole moment of a Kerr BH, but when $q \neq 0$ also the higher-order mass-multipole moments have a different value

² A self-gravitating fluid is expected to be symmetric with respect to the equatorial plane. In this case, all the α_n with n odd must vanish and the $n = 2$ and 4 are the two possible independent leading order corrections to the Kerr geometry of the MN metrics (in the MN solutions, the current moments are not independent; e.g. the current-octupole moment is set by the mass-quadrupole moment).

than in Kerr. For this reason, h measures the deviation from the hexadecapole moment of a Kerr BH only when $q = 0$.

The relation between prolate spheroidal and quasi-cylindrical coordinates is given by

$$\rho = k\sqrt{(x^2 - 1)(1 - y^2)}, \quad z = kxy, \quad (15)$$

with inverse

$$\begin{aligned} x &= \frac{1}{2k} \left(\sqrt{\rho^2 + (z+k)^2} + \sqrt{\rho^2 + (z-k)^2} \right), \\ y &= \frac{1}{2k} \left(\sqrt{\rho^2 + (z+k)^2} - \sqrt{\rho^2 + (z-k)^2} \right). \end{aligned} \quad (16)$$

The standard Boyer-Lindquist coordinates (r, θ) are related to the prolate spheroidal coordinates and the quasi-cylindrical coordinates by

$$\begin{aligned} r &= kx + M, \\ \cos \theta &= y, \end{aligned} \quad (17)$$

and

$$\begin{aligned} \rho &= \sqrt{r^2 - 2Mr + a_*^2 M^2} \sin \theta, \\ z &= (r - M) \cos \theta. \end{aligned} \quad (18)$$

Because the MN metrics are stationary and axisymmetric, geodesic orbits have two constants of motion, the specific energy $E = -u_t$ and the z -component of the

specific angular momentum $L_z = u_\phi$. The t - and ϕ -components of the 4-velocity of a test-particle are therefore

$$u^t = \dot{t} = \frac{Eg_{\phi\phi} + L_z g_{t\phi}}{g_{t\phi}^2 - g_{tt}g_{\phi\phi}}, \quad (19)$$

$$u^\phi = \dot{\phi} = -\frac{Eg_{t\phi} + L_z g_{tt}}{g_{t\phi}^2 - g_{tt}g_{\phi\phi}}. \quad (20)$$

where the dots denote derivatives with respect to the proper time. From the normalization of the 4-velocity $g_{\mu\nu}u^\mu u^\nu = -1$, we can write

$$\dot{\rho}^2 + \dot{z}^2 + V_{\text{eff}}(E, L, \rho, z) = 0, \quad (21)$$

where the effective potential V_{eff} is defined by

$$V_{\text{eff}} = \frac{f}{e^{2\gamma}} \left[1 - \frac{E^2}{f} + \frac{f}{\rho^2} (L_z - \omega E)^2 \right]. \quad (22)$$

Due to stationarity and the axisymmetry, the study of the geodesic dynamics can be restricted on a meridian plane ($\phi = \text{const}$), which is implied by Eq. (22) as well. Moreover, the motion takes place inside a region defined by $V_{\text{eff}} \leq 0$ (left panel of Fig. 1), whose border is the curve of zero velocity (CZV) $V_{\text{eff}} = 0$ (right panel of Fig. 1).

Circular orbits on the equatorial plane must have $\dot{\rho} = \dot{z} = 0$, which implies $V_{\text{eff}} = 0$, and $\ddot{\rho} = \ddot{z} = 0$, which implies $\partial_\rho V_{\text{eff}} = 0$ and $\partial_z V_{\text{eff}} = 0$. This means that circular equatorial orbits are located at simultaneous zeros and extrema of the effective potential. The extrema shown in the left panel of Fig. 1 indicate the existence of these circular orbits, the minima A_{min} , C_{min} , and E_{min} indicate the existence of stable circular orbits, while the maxima B and D indicate the existence of unstable circular orbits. In order to calculate the positions of the circular orbits, we must also demand that the effective potential to be equal to zero. Thus, because $\partial_z V_{\text{eff}} = 0$ is satisfied identically for $z = 0$ (simply because of the reflection symmetry of our MN metric with respect to the equatorial plane), from the aforementioned conditions one can obtain E and L_z as a function of the radius of the orbit ρ :

$$E = -\frac{g_{tt} + g_{t\phi}\Omega}{\sqrt{-g_{tt} - 2g_{t\phi}\Omega - g_{\phi\phi}\Omega^2}}, \quad (23)$$

$$L_z = \frac{g_{t\phi} + g_{\phi\phi}\Omega}{\sqrt{-g_{tt} - 2g_{t\phi}\Omega - g_{\phi\phi}\Omega^2}}, \quad (24)$$

where

$$\Omega = \frac{-\partial_r g_{t\phi} \pm \sqrt{(\partial_r g_{t\phi})^2 - (\partial_r g_{tt})(\partial_r g_{\phi\phi})}}{\partial_r g_{\phi\phi}} \quad (25)$$

is the angular frequency and the sign $+$ ($-$) is for orbits with angular momentum parallel (antiparallel) to the spin of the compact object. These orbits are stable under small perturbations in the radial direction if $\partial_\rho^2 V_{\text{eff}} > 0$, and in the vertical direction if $\partial_z^2 V_{\text{eff}} > 0$.

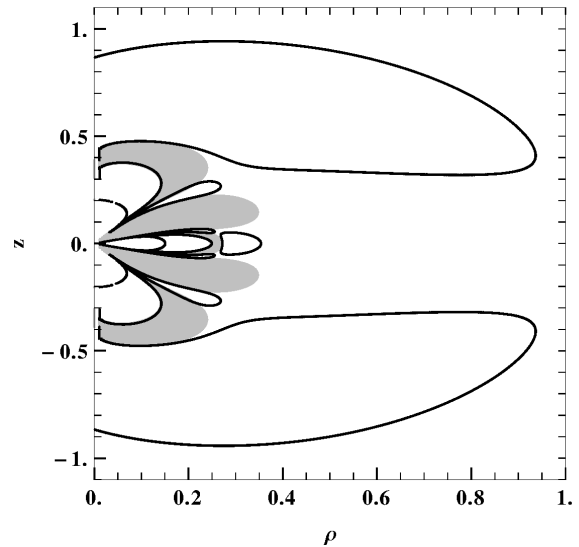


FIG. 2. The region with CTCs (in gray) is determined by the condition $g_{\phi\phi} < 0$, while the regions where motion is permitted are delimited by the CZV (black curves). It seems that the two regions never overlap for plausible values of the orbital parameters. The MN parameters, E , and L_z are the same as in Fig. 1.

The no-hair theorem [1] states that the only asymptotically flat, vacuum and stationary solution of the Einstein's equations that is non-singular on and outside an event horizon and that presents no closed time-like curves (CTCs) outside it is given by the Kerr metric. Therefore, the MN spacetimes must either have no event horizon, or present naked singularities or CTCs outside it. In fact, a MN metric can present the last two anomalies. Namely, the surface $x = 1$ ($\rho = 0, |z| \leq k$), which is the event horizon in the Kerr case $\alpha_n = 0$, is in general ($\alpha_n \neq 0$) only a partial horizon, because it presents a naked curvature singularity on the equatorial plane (i.e. at $x = 1, y = 0$, corresponding to $\rho = z = 0$). Moreover, there are CTCs outside it (Fig. 2). However, it seems that the CTCs and the allowed region $V_{\text{eff}} < 0$ do not overlap.

Nevertheless, in our scenario the exotic object is compact enough so that the plunging particles can reach the inner stable orbits, but not so much to have the region with CTCs. Furthermore, the pathological region with CTCs can even be removed by exciting the spacetime. This occurs, for example, if the spacetime goes to a new phase and a domain wall is formed [15, 16]. Across the domain wall, the metric is nondifferentiable and the expected region with closed timelike curves arises from the naive continuation of the metric ignoring the domain wall. The latter can be made of very exotic stuff, and in the literature there are examples of supertubes [15] and fundamental strings [16].

III. PROPERTIES OF EQUATORIAL CIRCULAR ORBITS IN MN SPACETIMES

A. MN spacetimes with $q \neq 0$ and $h = 0$

This is the case already discussed in the literature. The basic properties of equatorial circular orbits can be understood by considering a specific spin parameter a_* and by changing the anomalous quadrupole moment q . As an example, we report the values for the case $a_* = 0.5$ (see Tab. I).

For $q = 0$, we recover the Kerr spacetime. Outside the event horizon, the spacetime is everywhere regular (there are no CTCs). Circular orbits on the equatorial plane exist for radii $\rho > \rho_{PO}$, they are always vertically stable, but they are radially stable only for $\rho > \rho_{ISCO}$. If the compact object is surrounded by a thin accretion disk, the inner edge of the disk is at ρ_{ISCO} . For $a_* = 0.5$, we have $\rho_{PO} = 1.03$ and $\rho_{ISCO} = 3.11$ (here and in the following, we use units in which $M = 1$).

MN spacetimes with $q \neq 0$ have regions with CTCs just outside the event horizon. That is true even on the equatorial plane. When the compact object is more oblate than a Kerr BH ($q > 0$), there are no interesting new properties with respect to the Kerr metric. As the object becomes more and more oblate (q increases), the value of ρ_{ISCO} increases. For the case $q = 0.20$ shown in Tab. I, equatorial circular orbits exist for $\rho > 1.39$, they are always vertically stable, but they are radially stable only for $\rho > \rho_{ISCO} = 3.50$. Unlike the Kerr background, a narrow region with circular orbits appears even at very small radii ($\rho \approx 0.04$ for $q = 0.20$). This narrow region extends up to the region with CTCs. Even if it seems that this region never overlaps with the CTC region, it is more likely unphysical: these orbits have negative energy, suggesting that their possible existence would make the object unstable [17]. While orbits with negative energy exist even in the ergoregion of a Kerr BH, they are never stable.

For $q < 0$, the spacetime can have properties absent in the Kerr background and that are potentially of astrophysical interest. Let us consider again the example with $a_* = 0.5$. For small $|q|$, there is a region with circular orbits at small radii. Such orbits are radially stable, but vertically unstable. If we consider the case $q = -0.01$ of Tab. I, such a region is at $0.25 < \rho < 0.35$. At larger radii, circular orbits exist for $\rho > 0.99$, they are always vertically stable, but they are radially stable only for $\rho > \rho_{ISCO} = 3.09$. As $|q|$ increases, the size of the region with circular orbits at small radii increases as well, and eventually it merges with the one at larger radii. At this point, we have two disconnected regions with stable orbits, $\rho_1 < \rho < \rho_2$ and $\rho > \rho_{ISCO}$; this is the case of $q = -0.1$, with $\rho_1 = 1.00$, $\rho_2 = 1.16$ and $\rho_{ISCO} = 2.83$, and of $q = -0.2$, with $\rho_1 = 1.24$, $\rho_2 = 2.00$ and $\rho_{ISCO} = 2.17$. The orbit with radius $\rho = \rho_1$ is marginally unstable along the vertical direction, while the one with $\rho = \rho_2$ is marginally unstable along the ra-

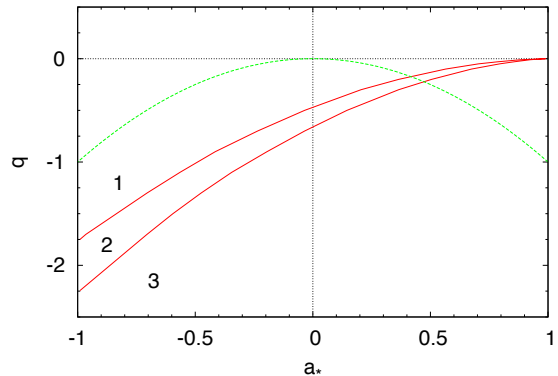


FIG. 3. MN spacetimes with non-vanishing anomalous quadrupole moment q . The solid red curves separate spacetimes with qualitatively different properties. Region 1: spacetimes in which equatorial circular orbits of astrophysical interest are located at $\rho > \rho_{ISCO}$ and the orbit at $\rho = \rho_{ISCO}$ is marginally stable along the radial direction. Region 2: spacetimes in which equatorial circular orbits of astrophysical interest are located at $\rho > \rho_{ISCO}$ and at $\rho_1 < \rho < \rho_3$ ($\rho_3 < \rho_{ISCO}$); the orbit at $\rho = \rho_1$ is marginally stable along the vertical direction, while the one at $\rho = \rho_{ISCO}$ is marginally stable along the radial direction; the energy of the orbits at $\rho = \rho_3$ and at $\rho = \rho_{ISCO}$ is the same and therefore the gas's particles can plunge from the inner edge of the external disk to the outer edge of the internal disk. Region 3: spacetimes in which equatorial circular orbits of astrophysical interest are located at $\rho > \rho_1$ and the orbit at $\rho = \rho_1$ is marginally stable along the vertical direction. The compact object is oblate if $q > -a_*^2$; the green dashed curve separates oblate objects from prolate objects. The compact object is more oblate than a Kerr black hole if $q > 0$. See the text for details.

dial direction. If the orbits in the region $\rho_1 < \rho < \rho_2$ have energy larger than the orbit at $\rho = \rho_{ISCO}$ (the case $q = -0.1$), the region $\rho_1 < \rho < \rho_2$ is not of astrophysical interest, as particles/gas orbiting around the compact object after reaching the radius ρ_{ISCO} plunge onto the compact object, without populating the region $\rho_1 < \rho < \rho_2$. However, as $|q|$ increases, the size of the region $\rho_1 < \rho < \rho_2$ also increases and there may exist a region $\rho_1 < \rho < \rho_3$ with $\rho_3 < \rho_2$ in which the orbital energy is smaller than the one at $\rho = \rho_{ISCO}$ (the case $q = -0.2$). These orbits are of astrophysical interest because they can be filled up by the gas of accretion reaching the radius $\rho = \rho_{ISCO}$. If $|q|$ continues increasing, the region $\rho_2 < \rho < \rho_{ISCO}$ with radially unstable orbits disappears: now circular orbits are always radially stable, but they are vertically stable for $\rho > \rho_1$, as is for the case $q = -0.3$, with $\rho_1 = 1.43$.

Fig. 3 shows the three different kinds of MN spacetimes with $q \neq 0$ on the plane spin parameter–anomalous quadrupole moment. The region 1, which includes the Kerr solution $q = 0$, has equatorial stable circular orbits for $\rho > \rho_{ISCO}$ and the orbit at $\rho = \rho_{ISCO}$ is marginally radially stable; for $q < 0$, these spacetimes may also

have equatorial stable circular orbits at smaller radii, but they are not of astrophysical interest because these orbits require energies higher than the one of the orbit at $\rho = \rho_{\text{ISCO}}$. In the region 2, there are spacetimes with equatorial stable circular orbits of astrophysical interest for $\rho_1 < \rho < \rho_3$ and $\rho > \rho_{\text{ISCO}}$ ($\rho_3 < \rho_{\text{ISCO}}$); the orbit at $\rho = \rho_1$ is marginally vertically stable, while the one at $\rho = \rho_{\text{ISCO}}$ is marginally radially stable. Lastly, the region 3 includes those spacetimes in which equatorial circular orbits are always radially stable, but they are vertically stable only for $\rho > \rho_1$.

B. MN spacetimes with $q = 0$ and $h \neq 0$

If the deformation parameter of the spacetime is the anomalous hexadecapole moment h instead of the q , the picture is qualitatively the same as the one discussed in the previous subsection, with h playing the role of $-q$ (the minus sign is just a matter of definition).

C. MN spacetimes with $q < 0$ and $h \neq 0$

Let us now discuss the more general scenario, when both q and h may be non-vanishing, starting from the case with $q < 0$. As in Subsection III A, we can consider the specific case $a_* = 0.5$ (see Tab. II); for another value of a_* , the picture is qualitatively the same, but the same phenomena occur for different values of q and h . First, we consider a spacetime in which $|q|$ is large enough that for $h = 0$ we have stable equatorial orbits for $\rho > \rho_1$. In Tab. II, we consider the specific case $q = -0.25$, where $\rho_1 = 1.34$ when $h = 0$. If we change the anomalous hexadecapole moment to $h = -0.03$, we find that circular orbits exist even in two narrow regions at small radii: a region close to the one with CTCs ($\rho \approx 0.27$), and another one in which the orbits are vertically stable but radially unstable ($0.40 < \rho < 0.43$). The latter expands as $|h|$ increases and it merges with the region of circular orbits at large radii. For instance, the regions $0.40 < \rho < 0.43$ and $\rho > 0.68$ for $h = -0.03$ become the region $\rho > 0.53$ when $h = -0.05$. At this point, we have three regions of stable circular orbits: one close to the pathological space with CTCs, one at $\rho_4 < \rho < \rho_5$, and the last one for $\rho > \rho_1$. The orbit at $\rho = \rho_4$ is marginally radially stable, while the one at $\rho = \rho_5$ is marginally vertically stable. For $h = -0.05$, the region close to the one with CTCs is at $\rho \approx 0.32$, while $\rho_4 = 0.67$, $\rho_5 = 0.70$, and $\rho_1 = 1.17$. A spacetime with similar properties does not exist if the only non-vanishing deformation parameter is q . Let us notice that the region $\rho_4 < \rho < \rho_5$ may include a subregion of astrophysical interest $\rho_4 < \rho < \rho_6$, where $\rho_6 < \rho_5$, in which the particles have energies smaller than the one of a particle at $\rho = \rho_1$. In presence of an accretion disk, the region $\rho_4 < \rho < \rho_6$ could be filled by the accreting gas. For larger values of $|h|$, the gap $\rho_5 < \rho < \rho_1$ disappears and stable orbits exist for $\rho > \rho_4$. This is the case

with $h = -0.08$, where $\rho_4 = 0.91$. By continuing to increase the value of $|h|$, a new gap shows up, in which the orbits are vertically stable but radially unstable. So, for $h = -0.1$ stable orbits exist for $\rho_4 < \rho < \rho_7$ and $\rho > \rho_8$, where $\rho_4 = 1.14$, $\rho_7 = 1.71$, and $\rho_8 = 2.04$. The new gap is $\rho_7 < \rho < \rho_8$ and we have used a different notation with respect to the gap $\rho_5 < \rho < \rho_1$ of the case $h = -0.05$ because it has different properties: ρ_7 and ρ_8 are marginally radially stable, while ρ_5 and ρ_1 were marginally vertically stable. If we continue increasing the value of $|h|$, the gap $\rho_7 < \rho < \rho_8$ disappears. This is the case $h = -0.15$: the spacetime now has features similar to that of a MN background with $q > 0$ and vanishing h , in which stable orbits exist for $\rho > \rho_4$ ($\rho_4 = 2.32$ for $h = -0.15$), the orbit at the radius $\rho = \rho_4$ is marginally radially stable, and the value of ρ_4 increases as $|h|$ increases.

If we start with $q = -0.25$ and $h = 0.0$ and we increase the value of h (now $h > 0$), we simply move ρ_1 at larger radii. For example, for $h = 1.0$ we have $\rho_1 = 2.06$, while for $h = 5.0$ we have $\rho_1 = 2.83$. We never form islands of stable circular orbits at small radii.

The properties of the MN spacetime may be even more interesting when q is still negative, but $|q|$ is not so large, so that for $h = 0$ the region $\rho_1 < \rho < \rho_2$ is still separated by a gap from the one $\rho > \rho_{\text{ISCO}}$. As a specific example, we have $q = -0.15$ in Tab. II. The properties of the equatorial circular orbits can be understood on the basis of the previous discussion. When $h = -0.01$, $\rho_1 = 1.08$, $\rho_2 = 1.40$, and $\rho_{\text{ISCO}} = 2.64$. For smaller h , we may have three disconnected regions of stable circular orbits (and, at least in some cases, of astrophysical interest): a new region at $\rho_9 < \rho < \rho_{10}$, the regions $\rho_1 < \rho < \rho_2$, and the one at $\rho > \rho_{\text{ISCO}}$. In the specific case $h = -0.029$, we find $\rho_9 = 0.68$, $\rho_{10} = 0.77$, $\rho_1 = 0.89$, $\rho_2 = 1.22$, and $\rho_{\text{ISCO}} = 2.67$.

D. MN spacetimes with $q > 0$ and $h \neq 0$

The properties of the case $q > 0$ can be easily expected on the basis of the results found in the previous subsections. The effect of increasing/decreasing h is equivalent to that of decreasing/increasing q . Tab. III shows the case $q = 0.25$.

E. Islands of stable equatorial circular orbits of astrophysical interest

The study of the previous subsections suggests the following conjecture: the MN spacetimes with arbitrary deformation parameters (q , h , and higher order deformations) can potentially have several disconnected regions with stable equatorial orbits of astrophysical interest. Accreting compact objects described by the MN solutions, if they exist, might thus be surrounded by Saturn-like structures, in which the accreting gas can fill different rings around the compact object. In the case $a_* = 0.5$,

a_*	q	h	Circular orbits	$\partial_\rho^2 V_{\text{eff}} > 0$	$\partial_z^2 V_{\text{eff}} > 0$	CTCs
0.5	0	0	$\rho > 1.03$	$\rho > 3.11$	$\rho > 1.03$	no CTCs
0.5	0.20	0	$\rho \approx 0.04$ $\rho > 1.39$	$\rho \approx 0.04$ $\rho > 3.50$	$\rho > 1.39$	$\rho < 0.04$
0.5	-0.01	0	$0.25 < \rho < 0.35$ $\rho > 0.99$	$0.25 < \rho < 0.35$ $\rho > 3.09$	$\rho > 0.99$	$\rho < 0.15$
0.5	-0.10	0	$\rho > 0.56$	$0.56 < \rho < 1.16, \rho > 2.83$	$\rho > 1.00$	$\rho < 0.35$
0.5	-0.20	0	$\rho > 0.73$	$0.73 < \rho < 2.00, \rho > 2.17$	$\rho > 1.24$	$\rho < 0.45$
0.5	-0.30	0	$\rho > 0.85$	$\rho > 0.85$	$\rho > 1.43$	$\rho < 0.52$

TABLE I. Regions with equatorial circular orbits (fourth column), radially stable orbits (fifth column), vertically stable orbits (sixth column), and CTCs (seventh column) in MN spacetimes with spin parameter $a_* = 0.5$, anomalous mass-quadrupole moment q , and vanishing anomalous mass-hexadecapole moment h . See the text for details.

a_*	q	h	Circular orbits	$\partial_\rho^2 V_{\text{eff}} > 0$	$\partial_z^2 V_{\text{eff}} > 0$	CTCs
0.5	-0.25	0.00	$\rho > 0.79$	$\rho > 0.79$	$\rho > 1.34$	$\rho < 0.49$
0.5	-0.25	-0.03	$\rho \approx 0.27$ $0.40 < \rho < 0.43$ $\rho > 0.68$	$\rho \approx 0.27$ $\rho > 0.68$	$\rho \approx 0.27$ $0.40 < \rho < 0.43$ $\rho > 1.26$	$\rho < 0.27$
0.5	-0.25	-0.05	$\rho \approx 0.32$ $\rho > 0.53$	$\rho \approx 0.32$ $\rho > 0.67$	$\rho \approx 0.32$ $0.53 < \rho < 0.70, \rho > 1.17$	$\rho < 0.32$
0.5	-0.25	-0.08	$\rho \approx 0.38$ $\rho > 0.69$	$\rho \approx 0.38$ $\rho > 0.91$	$\rho > 0.69$	$\rho < 0.38$
0.5	-0.25	-0.10	$\rho \approx 0.41$ $\rho > 0.77$	$\rho \approx 0.41$ $1.14 < \rho < 1.71, \rho > 2.04$	$\rho \approx 0.41$ $\rho > 0.77$	$\rho < 0.41$
0.5	-0.25	-0.15	$\rho \approx 0.45$ $\rho > 0.92$	$\rho \approx 0.45$ $\rho > 2.32$	$\rho > 0.92$	$\rho < 0.45$
0.5	-0.25	1.00	$\rho > 1.35$	$\rho > 1.35$	$\rho > 2.06$	$\rho < 0.87$
0.5	-0.25	5.00	$\rho > 1.88$	$\rho > 1.88$	$\rho > 2.83$	$\rho < 1.19$
0.5	-0.15	-0.010	$\rho \approx 0.21$ $0.30 < \rho < 0.31$ $\rho > 0.59$	$\rho \approx 0.21$ $0.59 < \rho < 1.40, \rho > 2.64$	$0.30 < \rho < 0.31$ $\rho > 1.08$	$\rho < 0.21$
0.5	-0.15	-0.029	$\rho \approx 0.30$ $\rho > 0.54$	$\rho \approx 0.30$ $0.68 < \rho < 1.22, \rho > 2.67$	$0.54 < \rho < 0.77, \rho > 0.89$	$\rho < 0.30$
0.5	-0.15	-0.035	$\rho \approx 0.32$ $\rho > 0.61$	$\rho \approx 0.32$ $0.80 < \rho < 1.13, \rho > 2.67$	$\rho > 0.61$	$\rho < 0.32$
0.5	-0.15	-0.050	$\rho \approx 0.36$ $\rho > 0.74$	$\rho \approx 0.36$ $\rho > 2.69$	$\rho > 0.74$	$\rho < 0.36$

TABLE II. Regions with equatorial circular orbits (fourth column), radially stable orbits (fifth column), vertically stable orbits (sixth column), and CTCs (seventh column) in MN spacetimes with spin parameter $a_* = 0.5$, anomalous mass-quadrupole moment $q < 0$, and anomalous mass-hexadecapole moment h . See the text for details.

$q = -0.15$ and $h = -0.029$, we can have an accretion disk with two internal rings. However, for non-vanishing higher order deformations, three or more rings may be possible.

IV. OBSERVATIONAL SIGNATURE

Let us consider a spacetime in which equatorial circular orbits are stable for $\rho > \rho_{\text{ISCO}}$ and in the inner regions $\rho_1 < \rho < \rho_2, \rho_4 < \rho < \rho_5$, etc. at smaller radii. In the presence of a gas of accretion, we may have the usual thin disk at $\rho > \rho_{\text{ISCO}}$ and several gas rings for $\rho_1 < \rho < \rho_3, \rho_4 < \rho < \rho_6$, etc. Is the thermal spectrum of this multi-

a_*	q	h	Circular orbits	$\partial_\rho^2 V_{\text{eff}} > 0$	$\partial_z^2 V_{\text{eff}} > 0$	CTCs
0.5	0.25	0.0	$\rho \approx 0.42$	$\rho \approx 0.42$		$\rho < 0.42$
			$\rho > 1.44$	$\rho > 3.58$	$\rho > 1.44$	
0.5	0.25	-1.0	$\rho \approx 0.77$	$\rho \approx 0.77$	$\rho \approx 0.77$	$\rho < 0.77$
			$\rho > 1.75$	$\rho > 3.79$	$\rho > 1.75$	
0.5	0.25	0.1	$0.59 < \rho < 0.67$	$0.59 < \rho < 0.67$		$\rho < 0.42$
			$\rho > 1.37$	$\rho > 3.55$	$\rho > 1.37$	
0.5	0.25	0.5	$\rho > 0.96$	$0.96 < \rho < 1.55, \rho > 3.43$	$\rho > 1.43$	$\rho < 0.67$
0.5	0.25	1.0	$\rho > 1.17$	$1.17 < \rho < 2.13, \rho > 3.21$	$\rho > 1.73$	$\rho < 0.79$
0.5	0.25	2.0	$\rho > 1.40$	$\rho > 1.40$	$\rho > 2.07$	$\rho < 0.93$

TABLE III. Regions with equatorial circular orbits (fourth column), radially stable orbits (fifth column), vertically stable orbits (sixth column), and CTCs (seventh column) in MN spacetimes with spin parameter $a_* = 0.5$, anomalous mass-quadrupole moment $q > 0$, and anomalous mass-hexadecapole moment h . See the text for details.

part accretion disk very different from the one we can expect around a Kerr BH with inner edge ρ_{ISCO}' ? The answer is no and the reason is the following. The high-energy part of the thermal spectrum of a thin accretion disk around a compact object depends on the radiative efficiency $\eta = 1 - E_{\text{in}}$, where E_{in} is the specific energy of the gas particles at the inner edge of the disk. So, it does not matter if the disk has some gaps. The thermal spectrum of our disk will look like the one around a Kerr BH with the same radiative efficiency. As the gas in inner rings necessarily has energy lower than the one at ρ_{ISCO} , the radiative efficiency of these objects is higher than $\eta = 1 - E_{\text{ISCO}}$, which might be (erroneously) interpreted as a higher value of the spin parameter of the object if we do not take the radiation from the inner disk into account. The ring structure of the accretion disk may be observed in high-resolution images of the disk itself, see e.g. Figs. 5 and 6 of Ref. [18], but this is definitively out of reach for present and near future facilities.

How can we then identify the existence of islands of stable orbits around a BH candidate? We think that a clear observational signature of these non-Kerr spacetimes may be found in the gravitational wave signal emitted by an extreme-mass ratio inspiral (EMRI) system, in which a stellar-mass compact object orbits around a super-massive BH candidate. In the standard case, the frequency and the amplitude of the waveform of the gravitational radiation are expected to increase regularly as the orbit of the small body shrinks to the ISCO radius – this is usually called the “chirp” phase in the literature. At the ISCO, the orbit becomes radially unstable and the stellar-mass body plunges into the super-massive BH candidate within a dynamical time-scale, emitting an irregular waveform. In the presence of inner regions of stable orbits, the picture may change as follows. As in the Kerr metric, the frequency and the amplitude of the waveform of the gravitational radiation should increase regularly as the small body approaches the ISCO radius. However, once at the ISCO, the small body may not plunge into the central object, but rather land in

an inner region with stable orbits. During the transition from the ISCO to the island, the system would emit some complicated waveform of gravitational waves to adjust the small body to the new orbit, but, after that, we should start observing again the typical EMRI waveform, in which the frequency and the amplitude increase regularly. This process may be repeated several times, with the small body that reaches the inner edge of an outer region and jumps to another region at smaller radii. The whole waveform should thus consist of several pieces of regular waveforms (the usual EMRI-type signal) broken by “bursts”, due to gravitational waves emitted when the small body adjusts into the new orbit.

Of course, our scenario can effectively work if the small body does jump from one region to another, without plunging directly into the central object. The correct approach to see if this is indeed the case is to compute the trajectory of one of these bodies including the radiation reaction. However, there is not an established prescription in the bibliography (at least to our knowledge) for handling radiation reactions in non-Kerr spacetimes. There are some tricks one can use in the relatively weak field limit [9, 10], but they cannot be used here, as in our case we are considering the region close to the compact object, where gravity is strong. Moreover, when the small body leaves the inner edge of a region of stable orbits, its trajectory is surely neither circular nor eccentric, and there might even be a chance that the orbit gets non-equatorial due to vertical instabilities, which makes the issue of radiation reaction even more difficult to handle in the strong regime. Therefore, in support of our scenario, we have simply checked if (in the geodesic approximation) the small body plunges quickly into the central one after having reached the ISCO radius or if it gets trapped in an inner region formed around circular orbits. Our numerical calculations show that the small body would indeed be trapped in an inner region, without plunging directly to the central object.

In the specific example we examined, we used a MN spacetime with parameters $M = 1$, $a_* = 0.5$, $q = -0.15$,

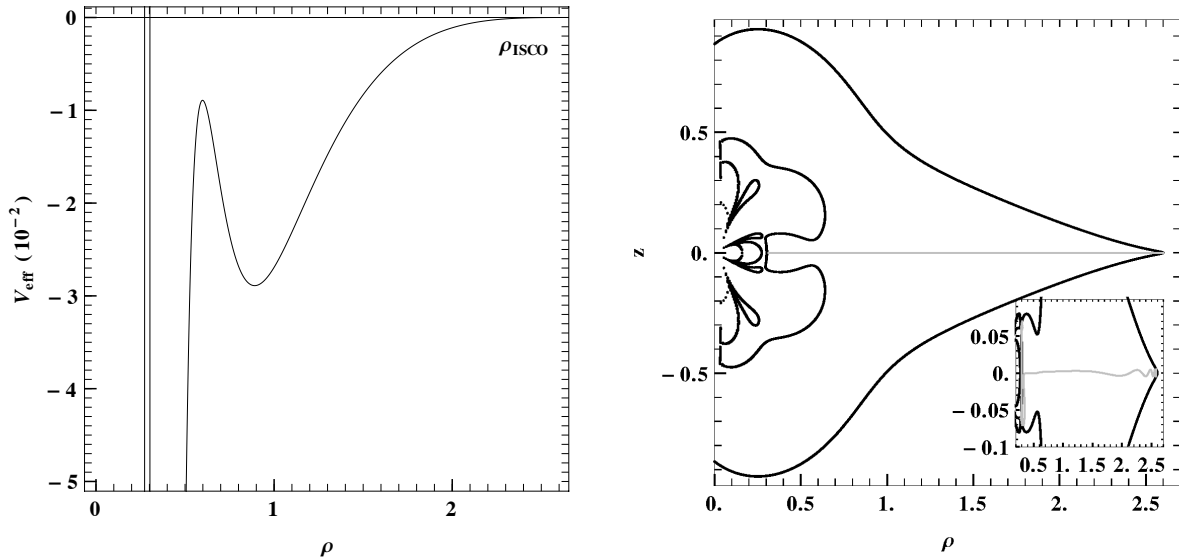


FIG. 4. The left panel shows the effective potential along ρ on the equatorial plane ($z = 0$) for the MN spacetime with parameters $M = 1$, $a_* = 0.5$, $q = -0.15$, and $h = -0.029$. The orbital parameters are $E = 0.911388$ and $L_z = 2.820706$, corresponding to the ones of a circular orbit at the ISCO radius. For the same spacetime and orbital parameters, in the right panel we show the CZVs (black curves) and an equatorial orbit ($z = \dot{z} = 0$) leaving the ISCO (the gray curve). In the embedded plot, the gray curve shows a non-equatorial orbit leaving the ISCO.

$h = -0.029$. The effective potential on the equatorial plane for energy and angular momentum corresponding to a circular orbit at the ISCO radius (left panel of Fig. 4) shows that between the ISCO and the horizon ($\rho = 0$) lies a deep potential well, which indicates the existence of stable circular orbits. On the $\rho - z$ plane in the right panel of Fig. 4, the CZVs (black curves) show the allowed region for an orbit leaving the ISCO. The deep well of the V_{eff} corresponds to the loop lying in the $0.3 < \rho < 0.6$ interval. If we evolve an equatorial geodesic orbit starting near $\rho = \rho_{\text{ISCO}}$, the orbit goes straight to the center of the well (gray curve in the right panel of Fig. 4), which means that it will be trapped for a while in the inner region of circular orbits, before the final plunge. If we now evolve a non-equatorial geodesic orbit starting near the ISCO radius, the orbit oscillates around the equatorial plane, but it also ends up in the well (embedded plot in the right panel of Fig. 4). Thus, even some vertical instabilities may not cause a direct plunge and may allow the small body to jump to an inner region of stable circular orbits. In the Kerr space-time, the particle cannot get trapped at small radii simply because there is no deep potential well between the object and the ISCO.

If we reduce the levels of energy and angular momentum, as would happen due to the radiation reaction, we find two marginally stable circular orbits, see Fig. 5. The first one is radially stable and vertically unstable and has orbital parameters $E = 0.888672$ and $L_z = 2.773112$. The second one is radially unstable and vertically stable, with orbital parameters $E = 0.796835$

and $L_z = 2.378980$. As the stellar-mass body leaves the ISCO radius, it loses energy and angular momentum. This changes the CZVs. In particular, the large allowed region in Fig. 4 may split. Depending on how the small body loses energy and angular momentum, it may adjust in the inner stable region at larger or smaller radii.

V. SUMMARY AND CONCLUSIONS

Astrophysical BH candidates are thought to be the Kerr BHs predicted by General Relativity, but this conclusion is not yet supported by robust observational evidence. In this paper, we discussed the observational implications in the case that BH candidates are exotic compact objects whose exterior gravitational field is described by the Manko-Novikov spacetimes, which are exact solutions of the vacuum Einstein's equations. Such a possibility is not in contradiction with current observations, but it requires some form of exotic matter beyond standard physics. However, the basic scope of our work is to provide an observational test of whether the centers of galaxies are occupied by Kerr BHs or by something more exotic, and not to argue that these exotic objects exist.

Equatorial circular orbits around a Kerr BH are always vertically stable, while they are radially stable only for radii larger than r_{ISCO} . The existence of stable equatorial circular orbits at radii smaller than r_{ISCO} in non-Kerr spacetimes was already known, but so far they have never

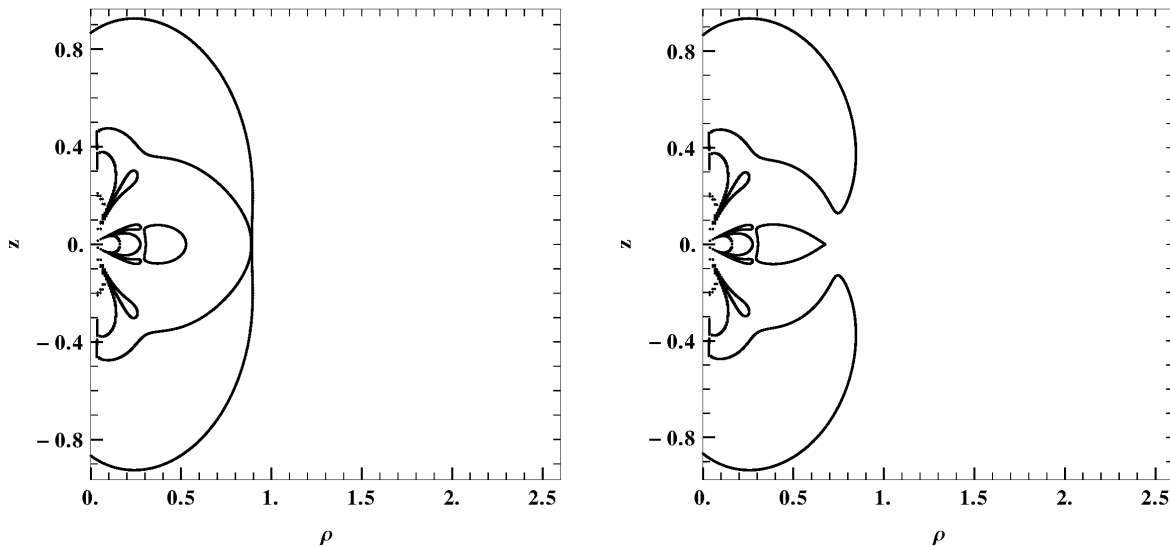


FIG. 5. The CZVs for the same spacetime parameters of Fig. 4 but for different orbital parameters. The left panel corresponds to $E = 0.888672$ and $L_z = 2.773112$, and the right to $E = 0.796835$ and $L_z = 2.378980$.

been considered to be of astrophysical interest as it was thought that their orbital energy was higher than the one at the ISCO and therefore that they could not be filled by the accretion gas or by small bodies inspiralling into the compact object. In this paper, we have pointed out that this is not always true. We have also argued that the maximum number of these non-plunging regions may increase as the structure of the spacetime becomes more and more complex by adding higher anomalous mass moments. Lastly, we have proposed that the existence of these regions of stable equatorial circular orbits around astrophysical BH candidates may be tested by observing the gravitational waves emitted by a stellar-mass compact object inspiralling into a super-massive BH candidate. In the standard case of a Kerr BH, the frequency and the amplitude of the waveform should regularly increase, in the so-called “chirp” of the system, up to the

plunging of the small body into the BH. In the presence of these inner regions, the total waveform could instead consist of “regular chirps”, produced when the stellar-mass compact object orbits in one of these stable regions, and “bursts”, necessary to adjust the small body to a new stable orbit of a more internal region. Such a signature in the waveform might be observed with future space-based gravitational wave detectors.

ACKNOWLEDGMENTS

We thank Enrico Barausse for reading a preliminary version of the manuscript and providing useful feedback. C.B. was supported by the Thousand Young Talents Program and Fudan University. G.L.G. was supported by the DFG grant SFB/Transregio 7.

-
- [1] B. Carter, Phys. Rev. Lett. **26**, 331 (1971); D. C. Robinson, Phys. Rev. Lett. **34**, 905 (1975).
[2] R. A. Remillard and J. E. McClintock, Ann. Rev. Astron. Astrophys. **44**, 49 (2006) [astro-ph/0606352].
[3] J. Kormendy and D. Richstone, Ann. Rev. Astron. Astrophys. **33**, 581 (1995).
[4] M. C. Miller and E. J. McColbert, Int. J. Mod. Phys. D **13**, 1 (2004) [astro-ph/0308402].
[5] C. E. Rhoades, Jr. and R. Ruffini, Phys. Rev. Lett. **32**, 324 (1974); V. Kalogera and G. Baym, Astrophys. J. **470**, L61 (1996) [astro-ph/9608059].
[6] E. Maoz, Astrophys. J. **494**, L181 (1998) [astro-ph/9710309].
[7] C. Bambi, Mod. Phys. Lett. A **26**, 2453 (2011) [arXiv:1109.4256 [gr-qc]]; C. Bambi, Phys. Rev. D **85**, 043002 (2012) [arXiv:1201.1638 [gr-qc]]; C. Bambi, Phys. Rev. D **86**, 123013 (2012) [arXiv:1204.6395 [gr-qc]]; C. Bambi, Astron. Rev. **8**, 4 (2013) [arXiv:1301.0361 [gr-qc]].
[8] V. S. Manko and I. D. Novikov, Class. Quant. Grav. **9**, 2477 (1992).
[9] J. R. Gair, C. Li and I. Mandel, Phys. Rev. D **77**, 024035 (2008) [arXiv:0708.0628 [gr-qc]].
[10] T. A. Apostolatos, G. Lukes-Gerakopoulos and G. Contopoulos, Phys. Rev. Lett. **103**, 111101 (2009) [arXiv:0906.0093 [gr-qc]]; G. Lukes-Gerakopoulos, T. A. Apostolatos and G. Contopoulos, Phys. Rev. D **81**, 124005 (2010) [arXiv:1003.3120 [gr-qc]].

- [11] C. Bambi and E. Barausse, *Astrophys. J.* **731**, 121 (2011) [arXiv:1012.2007 [gr-qc]]; C. Bambi, *Europhys. Lett.* **94**, 50002 (2011) [arXiv:1101.1364 [gr-qc]]. C. Bambi, *Phys. Rev. D* **83**, 103003 (2011) [arXiv:1102.0616 [gr-qc]]; C. Bambi, *JCAP* **1105**, 009 (2011) [arXiv:1103.5135 [gr-qc]]; C. Bambi, *Phys. Rev. D* **85**, 043001 (2012) [arXiv:1112.4663 [gr-qc]].
- [12] C. Bambi and E. Barausse, *Phys. Rev. D* **84**, 084034 (2011) [arXiv:1108.4740 [gr-qc]]; Z. Li and C. Bambi, *JCAP* **1303**, 031 (2013) [arXiv:1212.5848 [gr-qc]].
- [13] D. Pugliese, H. Quevedo and R. Ruffini, *Phys. Rev. D* **83**, 024021 (2011) [arXiv:1012.5411 [astro-ph.HE]]; D. Pugliese, H. Quevedo and R. Ruffini, *Phys. Rev. D* **84**, 044030 (2011) [arXiv:1105.2959 [gr-qc]].
- [14] G. Contopoulos, M. Harsoula and G. Lukes-Gerakopoulos, *Celest. Mech. Dyn. Astron.* **113**, 255 (2012); G. Lukes-Gerakopoulos and G. Contopoulos, (in preparation).
- [15] E. K. Boyda, S. Ganguli, P. Horava and U. Varadarajan, *Phys. Rev. D* **67**, 106003 (2003) [hep-th/0212087]; N. Drukker, *Phys. Rev. D* **70**, 084031 (2004) [hep-th/0404239]; E. G. Gimon and P. Horava, hep-th/0405019.
- [16] D. Israel, *JHEP* **0401**, 042 (2004) [hep-th/0310158].
- [17] P. Pani, E. Barausse, E. Berti and V. Cardoso, *Phys. Rev. D* **82**, 044009 (2010) [arXiv:1006.1863 [gr-qc]].
- [18] C. Bambi, *Astrophys. J.* **761**, 174 (2012) [arXiv:1210.5679 [gr-qc]].